Exposure Dose Optimization for a Positive Resist Containing Poly-functional Photoactive Compound

Peter Trefonas
Shipley Company
2300 Washington St.
Newton, MA 02162

Chris A. Mack
SEMATECH
2706 Montopolis Drive
Austin, TX 78741

Abstract

Methods for optimizing the photolithographic process with respect to exposure dose are described. Various latent image gradients (the photoactive compound gradient, $\partial m/\partial x$, the dissolution rate gradient, $\partial R/\partial x$, and the log dissolution rate gradient, $\partial lnR/\partial x$) at the mask edge in the resist film are compared as a function of exposure dose. The relationship between the sequential photochemical decomposition of poly-diazonaphthoquinone photoactive compound, dissolution models and the dissolution selectivity parameter n is discussed. A methodology using full scale simulation to explore the effect of exposure sizing dose upon resist profile sidewall angle, exposure latitude, focus range, and linewidth variation with resist thickness (swing ratio) is described and compared to simpler models based upon the use of latent image gradients. Finally, the correspondance between simulation and experiment is explored.

1. Introduction

Practical half-micron resolution microfabrication places stringent demands upon the photolithographic process. As a result, it becomes increasingly important that both the resist composition and the process are fully optimized in order to maximize lithographic performance. It is widely recognized that the optimum resist process is dependent on the resist composition, although the functionality of this dependence is not clearly understood. Recent studies have shown that one process parameter, the exposure dose required to give the nominal linewidth (called the dose to size, E_S), is a very important but often overlooked parameter needing optimization.

This paper will examine the role of exposure dose to size in determining process latitude. Using the lithography simulator PROLITH/2, the effect of E_S on resist profile sidewall angle, exposure latitude, focus range, and linewidth variation with resist thickness (swing ratio) will be examined. Comparisons will be made between simulated and experimental results in order to help validate the use of the model. The result will be a methodology with which to optimize the dose to size for a given resist material in order to maximize process latitude.

2. Background

The aerial image: The process of transferring a mask pattern into a photoresist pattern can be thought of as a transfer of information from the mask into the photoresist [1]. The information contained in the mask

0-8194-0565-5/91/$4.00

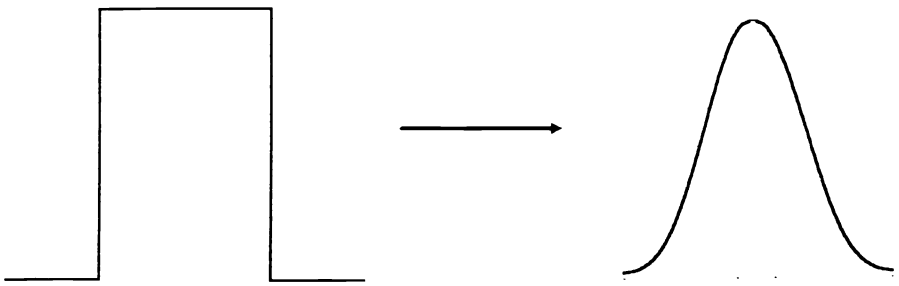

Figure 1. Information is lost when the mask pattern is converted into an aerial image by the optical projection system.

is the positions of the various edges. Consider, as the simplest example, a single space or line. The position of the two edges will, of course, define the width of the feature. The first step of the information transfer process is the projection of an image of the feature onto the wafer. The aerial image, $I(x)$, is not a perfect representation of the mask, as shown in Fig. 1. Diffraction limits the amount of information which can pass through the projection system, which in turn limits the information content of the image. The key information relating to the position of the edges in the aerial image can be characterized by the slope of the image at the mask edge, with a large slope meaning that the image does a good job of localizing this position. The quality of an aerial image can be quantified using the log-slope of the aerial image at the mask edge [2]:

$$I^{-1} \, \partial I / \partial x = \partial \ln(I) / \partial x \qquad (1)$$

(Note: Another metric of image quality is the log-slope multiplied by the width of the feature. This dimensionless metric is most useful when comparing different features which have linewidth specifications that are a fixed percentage of the nominal.)

It should be emphasized, however, that this method of analysis does not fullly characterize the entire information content of the aerial image. The aerial image log-slope and other quality metrics discussed later in this background are directed at characterizing the behavior of the image only at one location, namely the mask edge. Other lithographically important information concerning the aerial image, such as the relative image intensities at the masking locations corresponding to maximum and minimum illumination, are not addressed. As we will see later, conclusions drawn from analysis which characterize the aerial image at only one location may then be expected to differ somewhat from more complete methods.

The latent image: The next step in the information transfer process is the exposure of the photoresist with the aerial image. The exposure forms a distribution of exposed and unexposed photoactive compound (PAC) which is called the latent image, $m(x)$, where m is the relative concentration of unexposed photoactive compound (specifically, PAC will be defined in this paper as the photoactive diazonaphthoquinone (DNQ) moieties within the resist.) As with the aerial image, the latent image contains information about the position of the mask edges and this information can be characterized by the

latent image gradient at the mask edge. Knowing the kinetics of the exposure process, the latent image gradient can be related to the image log-slope. For a typical photoresist, the DNQ exposure kinetics are first order and the latent image gradient is given by [3]:

$$\partial m/\partial x = m\ ln(m)\ \partial lnI/\partial x \qquad (2)$$

Thus, the information content of the latent image is directly related to the information content of the aerial image. The term $m\ ln(m)$ is exposure dependent. This simple observation has far-reaching consequences. If the quality of the latent image can be judged by the latent image gradient, then the latent image quality is dose dependent. Consider the two extremes of exposure: zero dose and infinite dose. At these two extremes the latent image gradient is zero, as is the amount of information transferred. Since we known that the gradient is non-zero at some energy, it follows that there must be an optimum dose which maximizes the latent image gradient. Fig. 2 shows how the latent image gradient varies with exposure dose. There is an optimum dose, that which gives $m = 0.37$ (i.e, a dose such that 63% of the photoactive compound has been converted.)

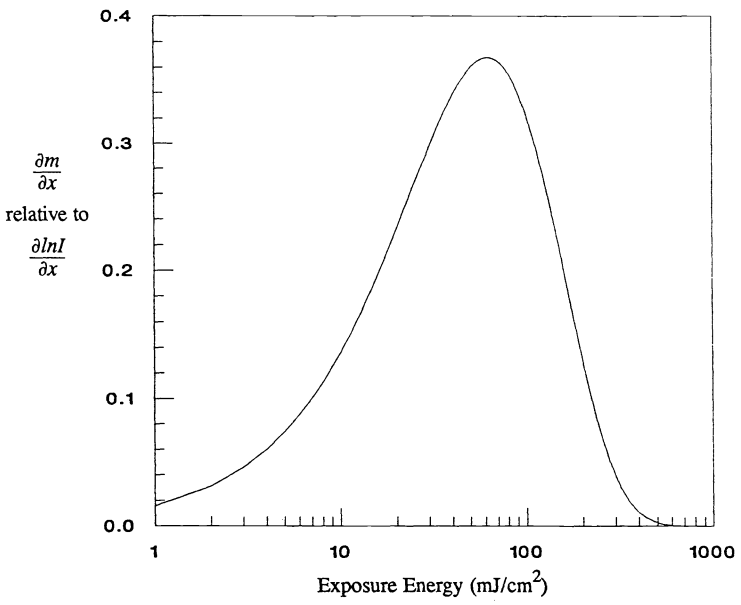

Figure 2. Variation of the latent image gradient (relative to the aerial image log slope), m ln(m), as a function of exposure dose.

Polyphotolysis and dissolution rate functions: In a resist where dissolution is related to a sequential photodecomposition of PAC, the dissolution response to irradiation can be supra-linear with respect to m [4-6]. This dissolution behavior can occur when poly-functional photoactive compounds with several DNQ groups per molecule (poly-PACs) are used in the resist, given the proper choice of resist materials and process. Poly-PACs undergo a sequential photochemical process during exposure to form a statistical mixture consisting of partially exposed molecules and fully exposed photoacid (with the distribution dependent upon exposure dose):

$$m_4 \xrightarrow{h\nu} m_3 \xrightarrow{h\nu} m_2 \xrightarrow{h\nu} m_1 \xrightarrow{h\nu} m_0$$

Example 1: Photolysis of PAC with initial composition consisting of four DNQ groups per molecule. Subscripts indicate the number of surviving DNQ groups on the molecule.

Multiple latent images in the resist film can arise from patternwise exposure as a result of the gradients corresponding to the concentrations of each individual photoproduct m_3 through m_0. A theoretical and experimental basis for improving resist performance through using a development process selective to the latent image(s) corresponding to poly-indenecarboxylic acid latent specie(s) has been described earlier [polyphotolysis: 6].

From the photochemical rate equations, it can readily be shown [6] that the poly-acid photoproduct concentration is related to dose according to:

$$m_0 = (1-e^{-EC})^q \qquad (3)$$

where E = exposure dose
C = the photochemical cross-section
and q = the original number of DNQ per molecule

Many modern positive DNQ resist systems display a dissolution rate behavior for which a simple best fit equation follows an equation very similar form [5-9] (see *Experimental*):

$$Rate = R_{max}(1-e^{-EC})^n + R_{min} \qquad (4)$$

where R_{max} = the fully exposed dissolution rate
n = the operant dissolution selectivity - "the *effective q*"
R_{min} = the unexposed dissolution rate

The exponent n controls the degree of curvature in the rate response to exposure dose; i.e. how fast resist dissolution "turns on". With careful selection of polymers, PACs and resist process, $n = q$ [6]. In practice, n can be significantly greater than q [10], or n can be much less than q (if intermediate photoproducts contribute significantly to resist dissolution) [6,11]. The similarities between eqs. 3 and 4 suggest that the dissolution rate equation could be recast as:

$$Rate = R_{max}\, m_0 + R_{min} \qquad (5)$$

where m_o = the *effective* photoacid concentration

Development rate gradients: The formation of a latent image is an intermediate step. The information contained in the latent image must be translated into a variation in development rate in order to form the final photoresist profile. Knowing the variation in development rate as a function of PAC concentration, one can translate a latent image concentration gradient into a development gradient. From equation (4) it is easy to derive the development rate gradient [12].

$$\partial R/\partial x = n * m\, lnm * (1-m)^{-1}\, (R - R_{min})\, \partial lnI/\partial x \qquad (6)$$

Like the latent image gradient, the development gradient is exposure dependent. There is one exposure

energy which gives the maximum development rate gradient. This optimum exposure, however, is dependent on the developer selectivity n. The dissolution selectivity is, in turn, a function of the composition of the resist material [6]. Fig. 3 is an example of this dependence when R_{max} = 160 nm/s, R_{min} = 0.1 nm/s, and n=5.

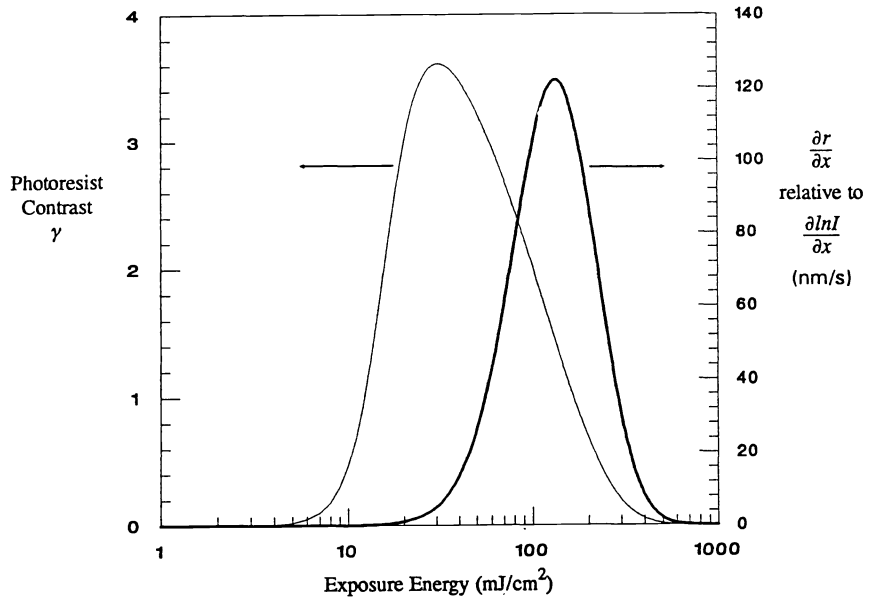

Figure 3. Variation of the development rate gradient and the log-development gradient (both relative to the aerial image log-slope) as a function of exposure dose.

<u>Resist Contrast:</u> One could argue that it is the logarithmic derivative of the development rate which is most important in lithography. This argument comes from the definition of photoresist contrast, γ [3]:

$$\gamma = \partial lnR/\partial lnE \tag{7}$$

From equation (7), it is easy to show that the log-development rate gradient and the log-slope of the aerial image are related by the photoresist contrast.

$$\partial lnR/\partial x = \gamma\, \partial lnI/\partial x \tag{8}$$

Thus, contrast can be thought of as the means of transferring information from the aerial image into the development rate differential required to obtain a resist profile. Equation (4) can be put into the form of a log-development rate gradient by dividing by the development rate:

$$\partial lnR/\partial x = n * m\, ln(m) * (1\text{-}m)^{-1} * (1\text{-}R_{min}/R)\, \partial lnI/\partial x \tag{9}$$

Thus, an expression for the contrast can be obtained by comparison of equations (8) and (9). Like equation (6), the photoresist contrast is exposure dependent and this dependence is a function of the value of the developer selectivity n [13] (Fig. 3).

The analysis presented above shows several very important properties of a lithographic process. First, imaging a photoresist can be thought of as a transfer of information. A common element through every equation presented above is the log-slope of the aerial image. The image log-slope is the information driver of the lithographic process. The exposure and development processes add an exposure dependence to the information transfer process. There is an optimum exposure which maximizes the information transfer into the photoresist, and this optimum is dependent on the developer selectivity parameter n. However, this analysis alone is not sufficient to determine exactly what the optimum exposure is for a given photoresist.

3. Exposure dose optimization from lithographic simulations

The simpler approaches to exposure dose optimization described in the earlier sections are useful in examining various gradients at specific locations within the resist film, such as the mask edge. However, during the course of resist development, each point on the final profile surface is the result of dissolution etching through all of the previous points within the film along the dissolution path. As such, the final location of an individual point on the final profile surface will be affected not only by the gradient at one particular location (e.g., the mask edge), but also by the gradients at each point along the entire dissolution path.

Lithographic simulation of the resist exposure and development processes is a technique which analyzes latent image information along the entire dissolution path in the determination of the resultant profile. Thus, a good simulator can offer the opportunity to optimize lithographic processes with respect to exposure dose in a much more complete manner. This direct approach will require that the aerial image $\partial I/\partial x$ be specified; in this paper we will examine exposure optimization for a process using a 0.45 NA i-line wafer stepper. The accuracy of these simulations to model a real resist was verified, and details are given in a later section.

Simulation methods: Simulations were performed using an advanced commercially available simulation package, PROLITH\2 (Macintosh version). Aerial images used are: wavelength = 365 nm; NA = 0.45; coherence = 0.5; fixed defocus = -0.3 μm; flare = 0; 0.5 μm lines in a 1.0 μm grating (sections 3.3 to 3.5) and 0.45 μm lines in a 0.9 μm grating (section 3.6 and 5.2). Resist parameters are: thickness =1.08 μm (variable in section 3.5); A = 0.85; B = 0.05; C = 0.016 and refractive index = 1.65. The substrate used is silicon; the post-exposure bake diffusion length was fixed at 40 nm. Development parameters are: development time = 60 s; developer selectivity n = variable (n = 5 in section 3.6), relative surface rate = 0.5 and relative surface depth = 0.1. The PAC concentration threshold (m_{th}) was set at m_{th} = -10 in order to make the dissolution rate equation used in PROLITH\2 be equivalent to equation 4.

Definition of sizing dose, E_S, and method for varying E_S: The exposure dose required to form a linewidth equal to the nominal mask linewidth, the sizing dose E_S, was adjusted by varying R_{max} and R_{min}, while keeping the ratio R_{max}/R_{min} = 1600. This technique of varying R_{max} and R_{min} should approximately simulate the effect of varying developer normality or resin dissolution rate on E_S. The ratio R_{max}/R_{min} was kept fixed in order to minimize the number of variables which will affect resist performance. The value used for this ratio, 1600, was arbitrary, but was felt to be reasonably

representative of many commercial resists. For purposes of illustration, the dose to size E_S will be discussed in energy units; it can also be expressed as the more general unitless parameter m (the photochemical cross-section parameter C was fixed at $C = 0.016$ cm^2/mJ in our simulations.)

Profile Sidewall Angle vs. E_S: Figure 4 shows the simulated relationship between resist sidewall angle and E_S as the resist dissolution selectivity factor n is varied. When the dose is greater than about 100 mJ/cm^2, as n increases, the sidewall angle improves. The gain in wall angle is the greatest as n is increased from $n = 1$ to $n = 2$; at higher n-values, the rate of improvement decreases. This response is in agreement with previously published observations [6].

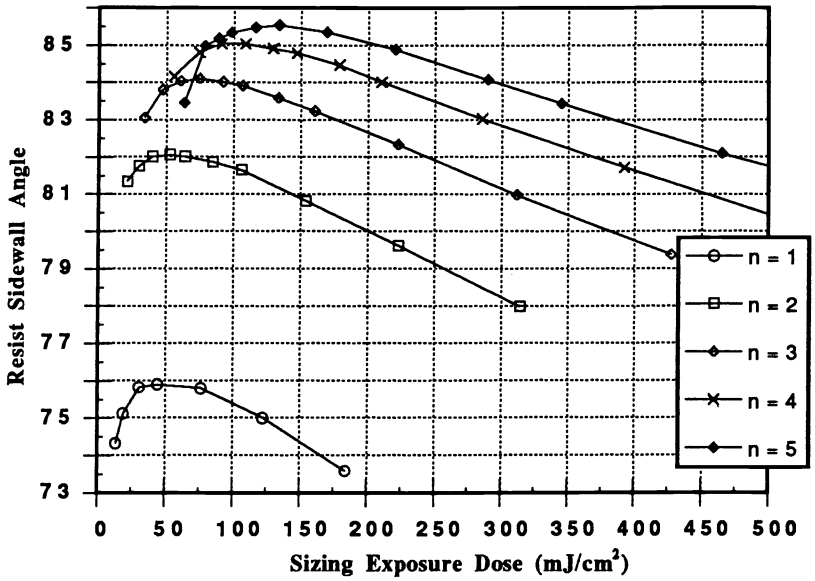

Figure 4. Plot of simulated resist sidewall angle vs. the sizing exposure dose as the resist dissolution selectivity is varied.

There is an exposure dose at which this sidewall angle response is optimum; this optimum dose increases from E_S = 45 mJ/cm^2 (m = 0.49) for n = 1 to E_S = 135 mJ/cm^2 (m = 0.11) for n = 5. The simulation results indicate that at low E_S, it may be preferable to chose a process which operates at $n = 2$ or $n = 3$; however at higher doses, the improving dissolution selectivity n will always lead to improved sidewall angle.

Exposure latitude vs. E_S: For purposes of discussion here, we have used a definition of normalized % exposure latitude (%EL) which is currently common in photolithographic engineering: the total deviation in exposure dose which produces a linewidth change of ±10% divided by the dose which yields a linewidth equal to the nominal linewidth, E_S. The relationship between %EL and E_S at different dissolution selectivity factors is shown in Figure 5.

The %EL response is similar to the sidewall angle response shown in the previous figure. At doses higher than 100 mJ/cm^2, improving the dissolution selectivity from n = 1 to n = 5 improved the %EL significantly. Unlike sidewall angle, the improvement in %EL with n seems to be rather constant,

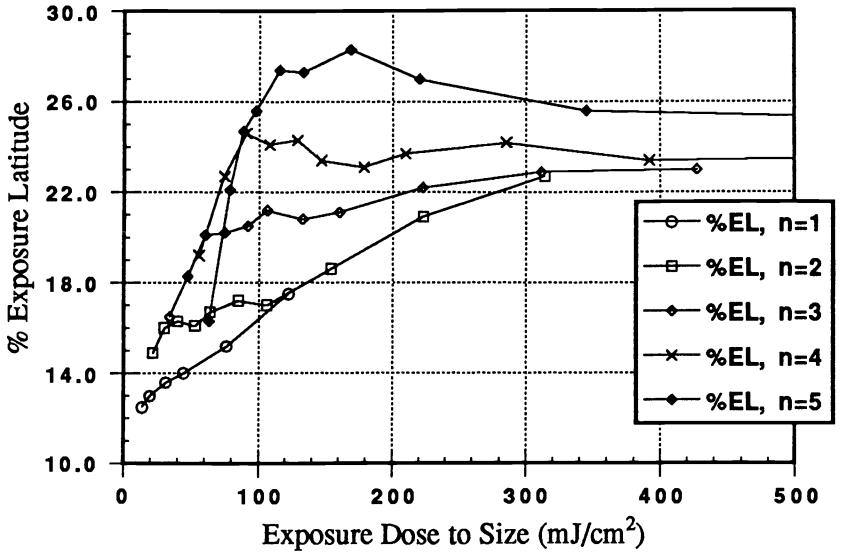

Figure 5. Plot of simulated percent exposure latitude vs. the sizing exposure dose as the resist dissolution selectivity is varied.

instead of dropping off at the higher n-values. The dose which optimizes %EL increases from E_S = 110 mJ/cm^2 (m = 0.17) for n = 3 to E_S = 170 mJ/cm^2 (m = 0.07) for n = 5. However, at lower dissolution selectivities (n < 3), %EL gradually increases as E_S increases and resists with lower n may yield a better %EL than resists with higher n. The difference in %EL response as dissolution selectivity is varied may be result from the built-in contrast enhancing effect of resist bleaching [14]. When $n \leq 2$, the resist can just barely resolve the 0.5 μm lines (and with a low sidewall angle), so the contrast enhancing effect with increasing dose plays a more significant role; at higher n, the benefits of this effect are less pronounced and the dissolution response predominates.

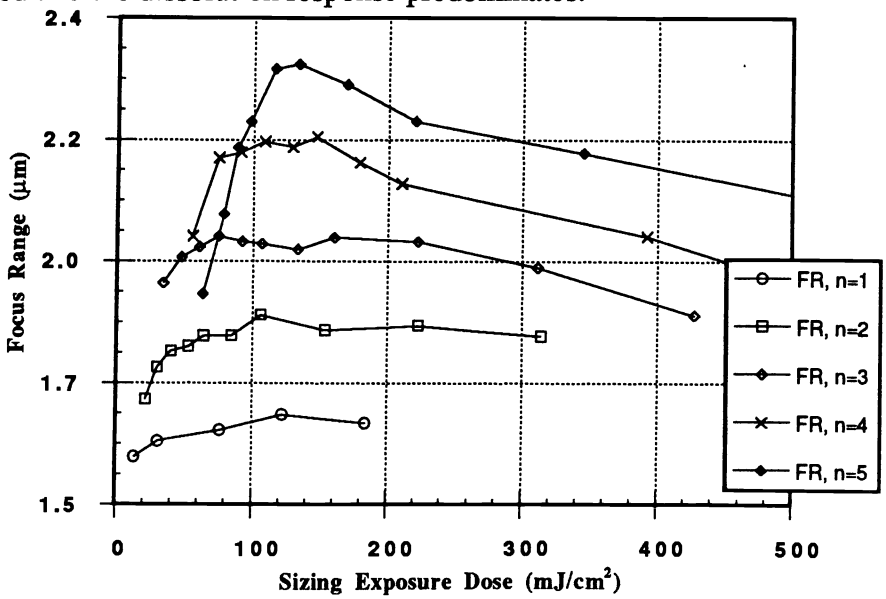

Figure 6. Plot of simulated focus range vs. the sizing exposure dose as the resist dissolution selectivity is varied.

Focus range vs. E_S: We again applied a common definition for focus range (FR): the range of focus deviation for which the linewidth remains within 10% of the nominal linewidth, with the exposure dose fixed at the dose to size, E_S. The relationship between focus range and E_S at different dissolution selectivities is shown in Figure 6.

The FR behavior is very similar to that of resist sidewall angle and %EL. Their appears to be a dose at which the FR is maximized for any particular n; this dose increases with increasing n. Because these curves cross, at very low E_S, resists with a lower E_S can have a better FR. At higher doses, FR increases with increasing dissolution selectivity. Similar to the behavior of %EL, the improvement of FR is rather constant with increasing n. The exposure dose which yields the optimum FR appears to remain rather constant with increasing n, at approximately E_S = 100 to 120 mJ/cm^2 (m = 0.20 to 0.15).

Linewidth swing ratio vs. E_S: Another important processing factor which can be strongly influenced by exposure dose is the resist "swing ratio". A plot of resist linewidth vs. film thickness is shown in Figure 7 from experimental work using Shipley Megaposit® SPR500™ photoresist. The linewidth swing ratio (%LW-SR) is determined from this periodic curve by taking amplitude of the linewidth, divided by the nominal linewidth, and expressing it on a percentage basis (at a specified film thickness.)

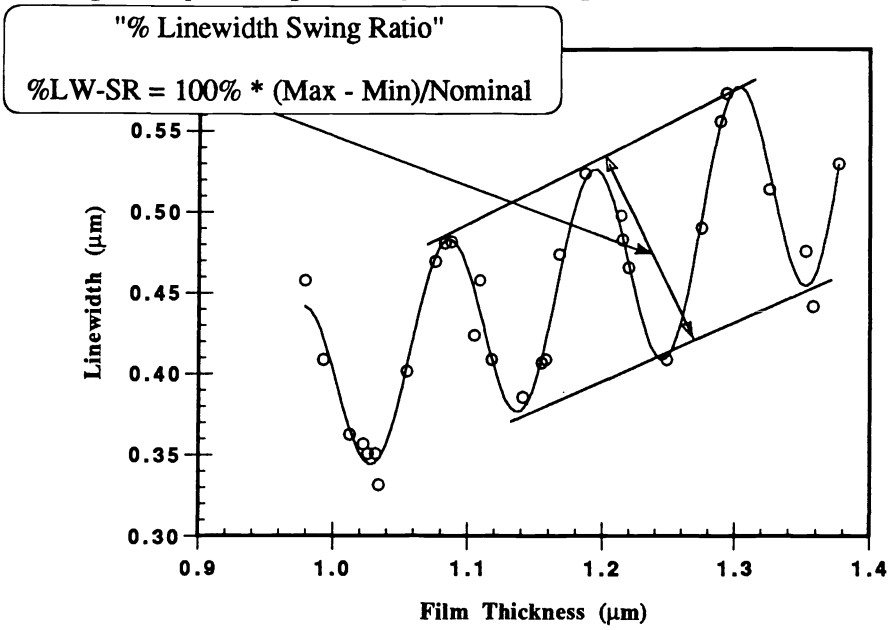

Figure 7. Plot of experimental linewidth vs. film thickness for Shipley SPR500 photoresist.

The swing ratio phenomena arises from variable amounts of light being coupled into the photoresist film as film thickness is varied. The amount of light coupled into the film changes as the reflectivity of the film stack varies; thus increasing resist film thickness causes periodic changes in reflectivity. Because linewidth is quite sensitive to the absorbed light dose, it will also show a similar periodic variation with changing film thickness [13].

The linewidth swing ratio is a function of two primary effects: resist absorbance (both bleachable and non-bleachable) and exposure latitude. First, at low absorbance, light is less attenuated as it is reflected

through the film, and as a result, more light is available to to couple periodically with changing film thickness, causing a larger %LW-SR. Second, as the exposure latitude worsens, and a larger change in linewidth will occur for a given change in absorbed light and %LW-SR should increase.

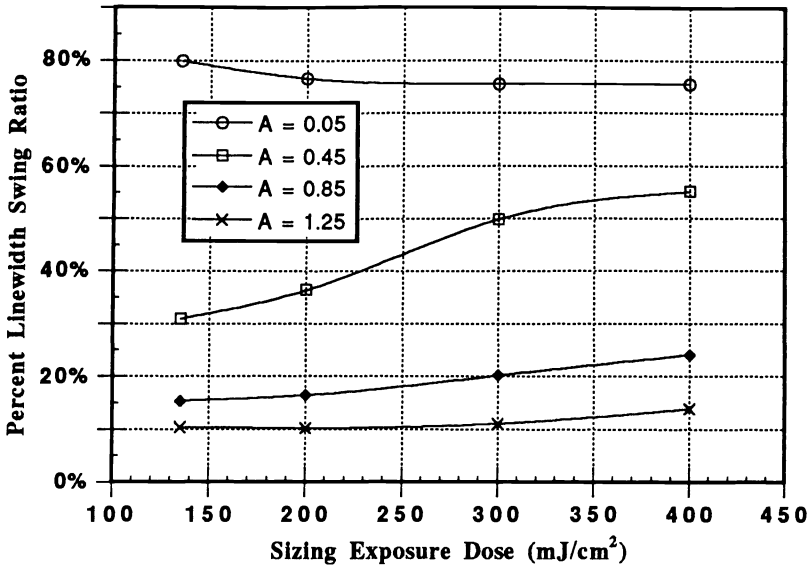

Figure 8. Simulated linewidth swing ratio as a function of resist A-parameter and dose.

Since exposure dose can significantly change both resist absorbance (assuming the resist can bleach) and exposure latitude, and therefore it is an important secondary variable which can influence the amplitude of the periodic linewidth variation. In Figure 8 a PROLITH\2 simulation is plotted of %LW-SR as a function of E_S and the resist A-parameter, while keeping other variables constant (among them, B = 0.05 and n = 5.) At low bleachable absorbance, A = 0.05, the %LW-SR is large, about 70 - 80%, which improves slightly with increasing E_S. This swing ratio is large because absorbance is low, so that the periodic variation with light coupling into the film is enhanced, resulting in large variations in linewidth. The slight improvement of %LW-SR at higher exposure doses is probably largely the result of improving exposure latitude. In contrast, at very high bleachable absorbance, such as A > 0.8, the %LW-SR is much smaller, about 10 - 20%, and becomes larger with increasing dose. Because initial absorbance is high, the periodic light coupling is reduced and the %LW-SR is smaller than the case where A is small. However, at higher exposure doses, the film becomes increasingly bleached and this effect is diminished, and %LW-SR increases (despite improving exposure latitudes.) At intermediate A-values (such as A = 0.45) the %LW-SR is very sensitive to E_S.

One can conclude from th the %LW-SR behavior that generally a lower E_S is preferred as it results in the smallest %LW-SR; lower exposure doses would be particularly preferred if A is of moderate magnitude (A = 0.3 to A = 0.65). The exception to this general trend occurs when the A-parameter is very small, in which case the %LW-SR is very large and is not significantly improved by changing exposure dose.

We did not examine the effects on %LW-SR of varying the non-bleachable absorbance (B-parameter) or adjusting the film thickness to be very thin (< 1 μm) or thick (>1.8 μm). Changing these variables could significantly affect the amount of light being absorbed by the film, and will likely have a significant impact on the %LW-SR. Another variable which remains to be studied is the influence of the resist

dissolution selectivity n; as was shown earlier, this significantly affects exposure latitude, and thus can be expected to impact %LW-SR.

4. Comparison of lithographic simulations with experiment

To a large extent, the accuracy of the conclusions drawn in this paper are dependent upon the accuracy of the fit of equation (4) to experimental rate data and the ability of PROLITH\2 to closely simulate the photolithographic process. In order to gain greater confidence in the modeling results, the dissolution rate response and the PROLITH\2 simulator were compared with experimental data.

Agreement between dissolution rate equation 4 and experimental rate data: Rate data was measured for several commercial resist materials using standard techniques [15] and plotted against the normalized diazonaphthoquinone content in the resist, m. In all cases , equation (4) gave a very good fit to the experimental data ($r > 0.97$). Data for three resists, along with the fit to equation (4) is shown in Figure 9.

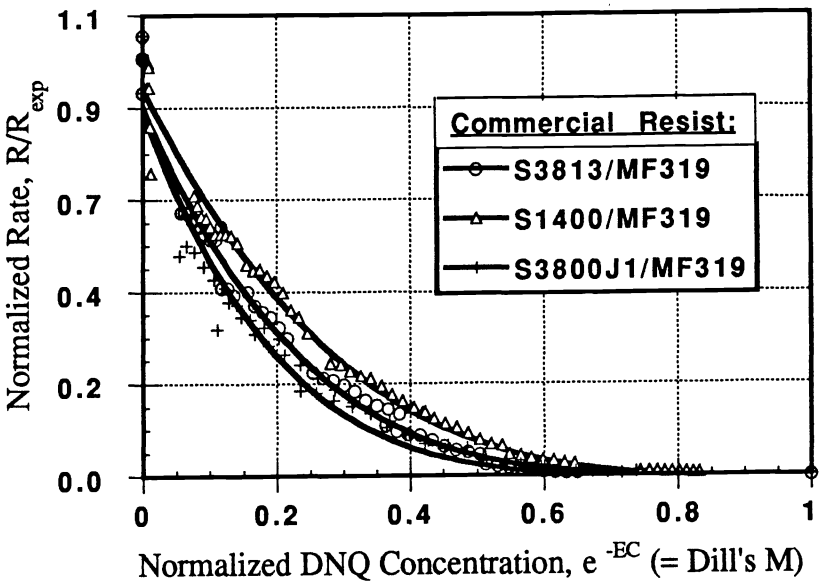

Figure 9. Plots of normalized dissolution rate vs. normalized resist diazonaphthoquinone concentration for Shipley Microposit© S3813™, S1400™ and S3800™ photoresists developed in Microposit© MF319™ developer fitted to equation 4. Data was obtained through standard techniques described in [15].

As an alternate (and simpler) technique, which is particularly useful for determining n, rate data is acquired on a 16-channel Perkin Elmer DRM. The dissolution rate R, at an arbitrary depth into the film (typically about 1/3 down into the film) is plotted against exposure dose E. R is then fit to E using equation (4), letting R_{max}, C and n vary, with R_{min} set at its experimental value (from the data set). By allowing C to vary, it is unnecessary to know the local dose corresponding to that depth into the film, since the effective dose will be the product CE. R is then plotted against e^{-CE} using the fitted value for C. The result is illustrated in Figure 10 for Megaposit© SPR500™ exposed using a HTG printer with a 15 nm i-line bandwidth filter, using a lithographic process otherwise identical to that described below.

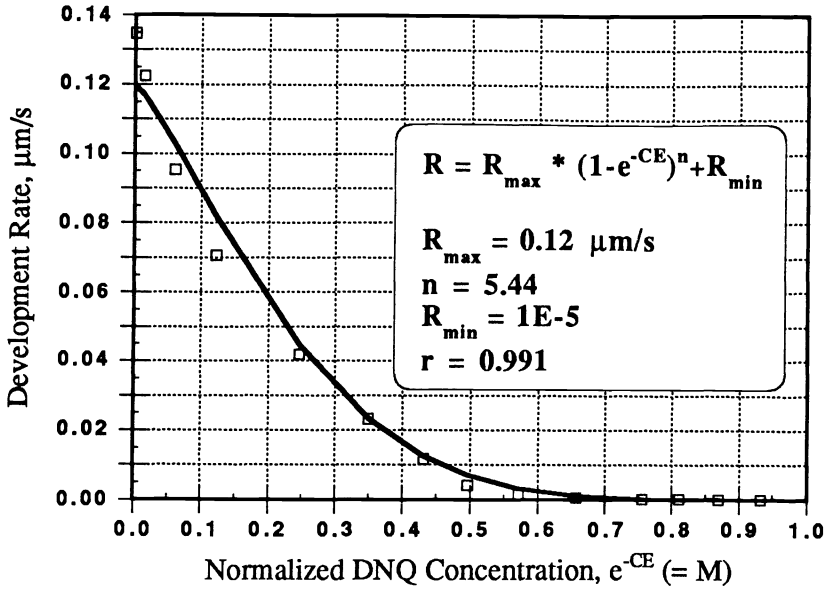

Figure 10. Plot of normalized dissolution rate vs. normalized resist diazonaphthoquinone concentration for Shipley Megaposit© SPR500™ photoresist developed in Megaposit© MF CD-26™ developer. Data was obtained through methods describe in section 4 using a Perkin Elmer DRM.

Comparison between PROLITH\2 simulation and experiment: Key lithographic responses, such as profile shape, focus and exposure latitudes, and mask-matching linearity were compared for the commercial resist SPR500 and the PROLITH\2 simulator. The SPR500 resist was processed using a softbake of 90°C/60s, exposed on a 0.45 NA i-line GCA stepper, post-exposure baked at 110°C/60s and developed in 0.26 N aqueous tetramethylammonium hydroxide using conventional track equipment. The parameter set used in PROLITH\2 is discussed earlier in section 3, with the flare set at 1%. R_{max}, C, n and R_{min} were determined as described above.

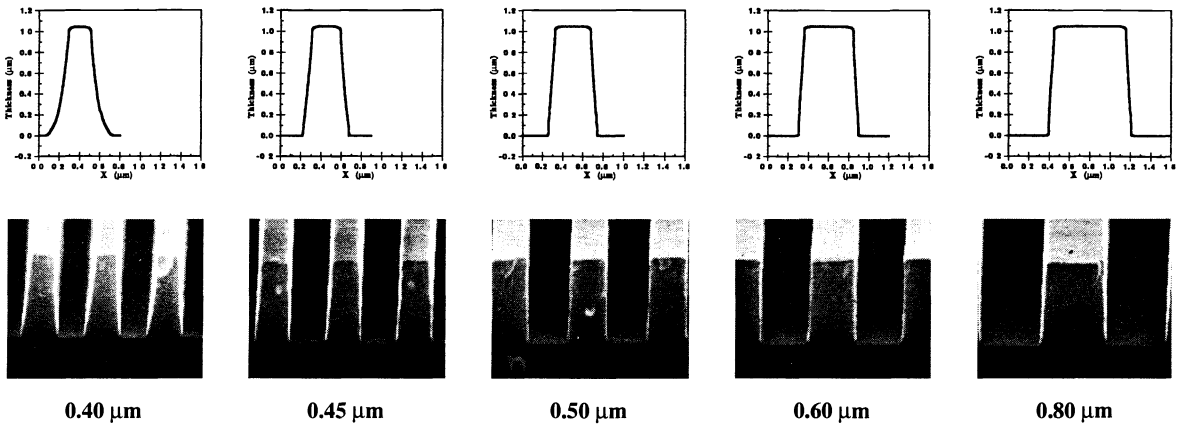

Figure 11. Simulated vs. experimental profiles as linewidth is varied for Shipley SPR500 photoresist.

Resist profiles from both experiment and simulation of 0.4 to 0.8 µm nominal linewidths are shown in

Figure 11. A mask-matching linearity plot of actual linewidth vs. nominal linewidth for the same profiles is shown in Figure 12. The correspondence is excellent. The major difference between experiment and simulation was the sizing dose required to print these features, E_S = 133 mJ/cm^2 (experimental) vs. 162 mJ/cm^2 (simulation). This discrepancy could however easily result from several factors, the most significant of which are suspected to be: 1. differences/errors in dose calibration of the lamps used in the stepper and the exposure equipment used to gather the dissolution rate data; 2. different spectral bandwidths between the exposure tools; 3. environmental changes (the wafers were processed at different locations); 4. errors in fitting the thickness data to equation 4 (particularly the C-value); and 5. approximations associated with the models used in the PROLITH\2 simulator.

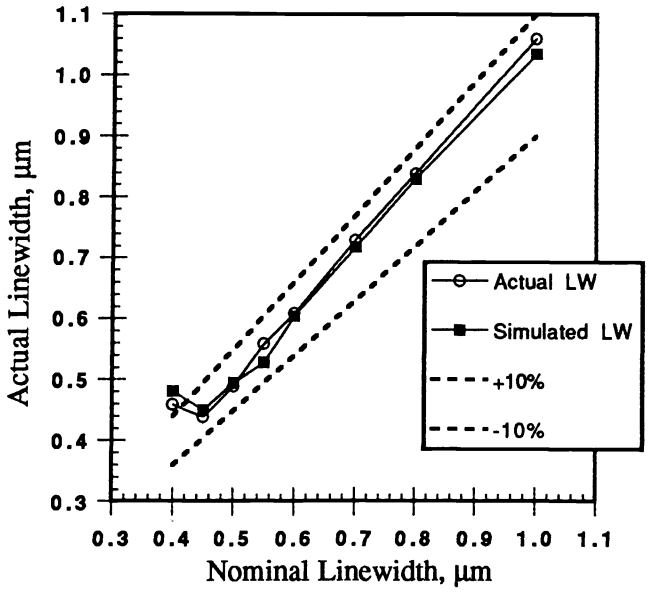

Figure 12. Plot of actual vs. nominal linewidths for the resist profiles in Figure 11.

Exposure and focus latitudes for 0.45 µm line/space gratings are compared in Figure 13. The correlation between experiment and simulation for %EL is very good, 23.6% vs 20.5%, respectively. The correlation for FR is less close, 1.5 µm (experiment) vs. 2.0 µm (simulation). The overestimation of focal range in the simulation relative to experiment is probably due primarily to lense defects, such as a significant astigmatism, which reduce the quality of the aerial image of projected by the exposure tool and limit the experimental depth of focus. The PROLITH\2 model assumes an ideal aerial image, to which some degradation can be added by including a background "flare term". Proper adjustment of the flare term could probably improve the correspondance between experiment and model. Nevertheless, the profile shapes as focus is varied are in reasonably good correlation with experiment.

5. Conclusions

The complexity of the interactions of the many optical and chemical variables which control profile shape and linewidth in microlithography makes process optimization difficult, even when the optimization of a single variable, e.g. exposure dose, is chosen. Simple methods, such as the analysis of intermediate results - various latent image gradients - predict that there will be an exposure dose which will optimizes certain lithographic responses. While full simulations also support that there will be an optimum

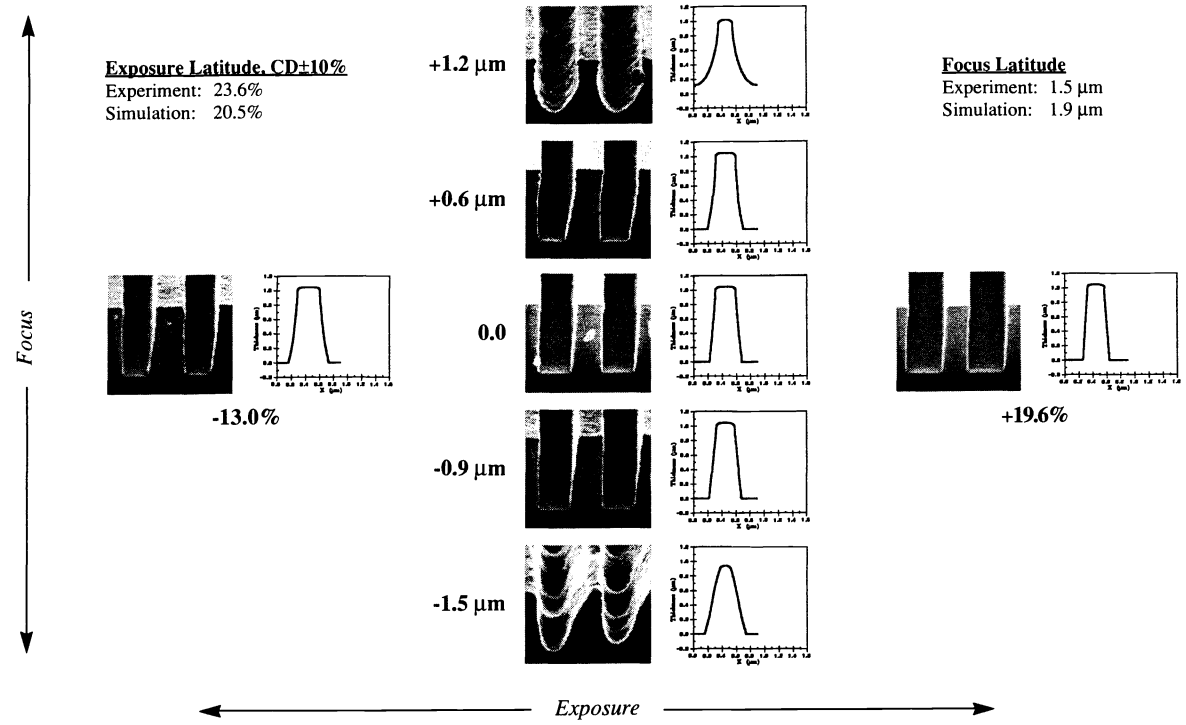

Figure 13. Simulated vs. experimental profiles as exposure and focus is varied for Shipley SPR500 photoresist.

exposure dose which optimizes lithographic responses such as profile wall angle, exposure and focus latitudes, the required exposure dose is significantly less than that predicted by the simpler methods.

In this paper, it has been shown that the choice of process exposure dose will significantly affect key processing latitudes. The optimum dose increases with resist dissolution selectivity n which is related, but not identical to, the number of photochemical sites per molecule. This behavior is in agreement with previous predictions concerning the use of poly-functional PACs which require multiple photochemical conversions before dissolution rate "turns on".

Finally, a methodology has be developed which allows the optimization of the lithographic process around key user-definable variables, such as exposure dose. While the key lithographic process parameters were (arbitrarily) chosen in this investigation to be profile sidewall angle, linewidth swing ratio, focus and exposure latitudes, other process parameters could have equally well been selected. More work will be required to determine how sensitive exposure dose is to other user definable variables: aerial image, film thickness, dye loading (B-parameter), etc. This methodology described here could be extended to the optimization of resist design by the selection of A and B-parameters, dissolution selectivity, R_{max} and R_{min}, etc.

Acknowledgements

The authors wish to thank and acknowledge R. Fischer, B. Andrews and J. Wickman for lithographic work on SPR500 resist, M. Perkins and P. Turci for dissolution rate measurements.

References

1. A discussion of the application of information theory to photolithography can be found in C.R.Szmanda and P.Trefonas, "Chemical Amplification in Submicron Lithography: An Information Theoretic Analysis," *Microcircuit Eng. 90*, (1990) in press.
2. C. A. Mack, "Understanding Focus Effects in Submicron Optical Lithography," *Optical/Laser Microlith., Proc.*, SPIE Vol. 922 (1988) pp. 135-148, and Optical Eng., Vol. 27, No. 12 (Dec. 1988) pp. 1093-1100.
3. C. A. Mack, "Photoresist Process Optimization," *KTI Microelectronics Seminar, Proc.*, (1987) pp. 153-167. Note that Mack's usage of m_0 differs from the usage in this paper.
4. The treatment of sequential photochemical reactions in a negative resist results in a similar model: P.D.Blais, "A Statistical Model for the Crosslink Density in Negative Type Photoresist Systems," *Kodak Interface*, (1975) pp. 6-15.
5. C. A. Mack, "PROLITH: A Comprehensive Optical Lithography Model," *Optical Microlith. IV, Proc.*, SPIE Vol. 538 (1985) pp. 207-220. The justification for eq. 28 in this paper derives from the implicit assumption of a strong PAC/resin (or photoproduct/resin) interaction. There is experimental justification for this possibility [10]. Mack's dissolution rate equation 31 becomes identical to eq. 4 when m_{th} is a large negative number.
6. P. Trefonas and B. K. Daniels, "New Principle for Image Enhancement in Single Layer Positive Photoresists," *Advances in Resist Technology and Processing IV, Proc.*, SPIE Vol. 771 (1987) pp. 194-210.
7. Another simulation of sequential chemical reactions, relating to crosslinking events in negative resist, is described in: R.A.Ferguson, J.M.Hutchison, C.A.Spence and A.R.Neureuther, "Modeling and Simulation of a Deep-UV Acid Hardening Resist," *J.Vac.Sci.Tech. B*, Vol. 8, No. 6 (1990) pp. 1423-1427.
8. Y.Hirai, et. al., "Process Modeling for Photoresist Development and Design of Double-Layer Resist by a Single Development Process," *IEEE Trans. on Computer Aided Design*, CAD-6, (1987) pp. 403-409.
9. M.Cagan, D.Kyser, C.Lyons, G.Hefferon and S.Miura, "Functional Evaluation and Simulation of Half-Micron High Contrast I-Line Processing on a 0.40 NA Exposure System," *Proc. KTI Interface Conf.*, (1990) pp. 177-215.
10. C.R.Szmanda, A.Zampini, D.C.Madoux and C.L.McCants, "Photoactive Compound Structure and Resist Function: Influence of Chromophore Proximity," *Proc. SPIE*, Vol. 1086, (1989), p.363.
11. S.Tan, S.Sakaguchi, K.Uenishi, Y.Kawabe and R.J.Hurditch, "Novel Diazonaphthoquinone Photoactive Compound for G-Line/I-Line Compatible Positive Photoresist," *Proc. SPIE*, Vol. 1262, (1990) p. 513.
12. P. Trefonas, T.A. Fisher, and J. Lachowski, "What is the Optimum Dose for a Positive Resist Containing Poly-functional Photoactive Compound?" *Microcircuit Engin. 90, Proc.*, (1990).
13. C. A. Mack, "Lithographic Optimization Using Photoresist Contrast," *KTI Microlithography Seminar, Proc.*, (1990) pp. 1-12, and *Microelectronics Manufacturing Technology*, Vol. 14, No. 1 (Jan. 1991) pp. 36-42.
14. K. Miura at al., "Masking Effect and Internal CEL, New Design Concepts for Positive Working Photoresists," *Proc. SPIE*, Vol 920 (1988) pp. 134-137.
15. D.J.Kim, W.G.Oldham and A.R.Neureuther, "Characterization of Resist Development: Models, Equipment, Method and experimental Results," *Kodak Interface*, (1982) pp. 1-15.